Journal Pre-proof

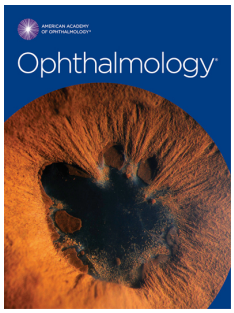

RP2-associated X-linked Retinopathy: Clinical Findings, Molecular Genetics, and Natural History.

Michalis Georgiou, Anthony G. Robson, Katarina Jovanovic, Thales Antônio Cabral De Guimarães, MD, Naser Ali, Nikolas Pontikos, Sami H. Uwaydat, Omar A. Mahroo, Michael E. Cheetham, Andrew R. Webster, Alison J. Hardcastle, Michel Michaelides

PII: S0161-6420(22)00916-2

DOI: https://doi.org/10.1016/j.ophtha.2022.11.015

Reference: OPHTHA 12257

To appear in: *Ophthalmology*

Received Date: 21 September 2022

Revised Date: 10 November 2022

Accepted Date: 10 November 2022

Please cite this article as: Georgiou M, Robson AG, Jovanovic K, Cabral De Guimarães TA, Ali N, Pontikos N, Uwaydat SH, Mahroo OA, Cheetham ME, Webster AR, Hardcastle AJ, Michaelides M, *RP2*-associated X-linked Retinopathy: Clinical Findings, Molecular Genetics, and Natural History., *Ophthalmology* (2022), doi: https://doi.org/10.1016/j.ophtha.2022.11.015.

RP2-associated X-linked Retinopathy: Clinical Findings, Molecular Genetics, and Natural History.

Michalis Georgiou[1,2,3], Anthony G. Robson[1,2], Katarina Jovanovic[2], Thales Antônio Cabral De Guimarães, MD,[1, 2] Naser Ali,[1, 2] Nikolas Pontikos,[1, 2] Sami H. Uwaydat[3], Omar A Mahroo[1,2], Michael E. Cheetham[2], Andrew R. Webster[1,2], Alison J. Hardcastle[2], Michel Michaelides[1,2] *

[1.] Moorfields Eye Hospital, London, UK
[2.] UCL Institute of Ophthalmology, University College London, London, UK
[3.] Jones Eye Institute, University of Arkansas for Medical Sciences, Little Rock, AR, USA.

***Correspondence / Reprints:**
Prof. Michel Michaelides,
UCL Institute of Ophthalmology, 11-43 Bath Street, London, EC1V 9EL, UK.
Email: michel.michaelides@ucl.ac.uk
Tel: +44 207 608 6864

Financial Support: MM supported by grants from the National Institute for Health Research Biomedical Research Centre at Moorfields Eye Hospital NHS Foundation Trust and UCL Institute of Ophthalmology, and The Wellcome Trust (099173/Z/12/Z). NP is currently funded by a NIHR AI Award (AI_AWARD02488).

Financial Disclosures: Michel Michaelides consults for MeiraGTx.
Conflict of Interest: No conflicting relationship exists for any author
Word Count (excluding title page, tables, references, and figure legends): 3252 words
Running Head: *RP2*-associated Retinopathy

Keywords: Phenotyping, Genotyping, Retinopathy, Inherited Retinal Diseases, Genetics, *RP2,* Retinitis Pigmentosa

ABSTRACT

Purpose:

To review and describe in detail the clinical course, functional and anatomical characteristics of *RP2*-associated retinal degeneration.

Design: Retrospective case series.

Participants

Males with disease-causing variants in the *RP2* gene.

Methods:

Review of all case notes and results of molecular genetic testing, retinal imaging (fundus autofluorescence (FAF) imaging, optical coherence tomography (OCT)) and electrophysiology assessment.

Main Outcome Measures

Molecular genetic testing, clinical findings including best-corrected visual acuity (BCVA), qualitative and quantitative retinal imaging analysis, and electrophysiology parameters.

Results

Fifty-four molecularly confirmed patients were identified, from 38 pedigrees. Twenty-eight disease-causing variants were identified; with 20 not previously clinically characterized. Fifty-three patients (98.1%) presented with retinitis pigmentosa. The mean age of onset (range, ±SD) was 9.6 years of age (1-57 years, ± 9.2 years). Forty-four patients (91.7%) had childhood-onset disease, with mean age of onset of 7.6 years. The commonest first symptom was night blindness (68.8%). Mean BCVA (range, ±SD) was 0.91 LogMAR (0-2.7, ±0.80) and 0.94 LogMAR (0-2.7, ±0.78) for right and left eyes respectively. Based on the WHO visual impairment criteria, 18 patients (34%) had low vision. The majority (17/22) showed ERG evidence of a rod-cone dystrophy. Pattern ERG P50 was undetectable in all but 2 patients. A range of FAF findings was observed, from normal to advanced atrophy. There were no statistically

significant differences between right and left eyes for ellipsoid zone (EZ) width and outer nuclear layer (ONL) thickness. The mean annual rate of EZ width loss was 219 µm/year and the mean annual decrease in ONL thickness was 4.93 µm/year. No patient with childhood-onset disease had identifiable EZ after the age of 26 years at baseline or follow-up. Four patients had adulthood-onset disease and a less severe phenotype.

Conclusions: This study details the clinical phenotype of *RP2* retinopathy in a large cohort. The majority presented with early-onset severe retinal degeneration, with early macular involvement and complete loss of the foveal photoreceptor layer by the third decade of life. Full-field ERGs revealed rod-cone dystrophy in the vast majority, but with generalised (peripheral) cone system involvement of widely varying severity in the first two decades of life.

Abbreviations/Acronyms: XLRP, X-linked Retinitis Pigmentosa; SD-OCT, Spectral Domain optical coherence tomography; FAF, Fundus autofluorescence; RPE, Retinal pigment epithelium; CFP, Color fundus photography; ISCEV, International Society for Clinical Electrophysiology of Vision; ERG, Electroretinogram; PERG, Pattern ERG; VF, Visual Field; SD, standard deviation; VA, visual acuity.

INTRODUCTION

Retinitis Pigmentosa (RP) is an heterogeneous group of inherited retinal conditions, both in terms of phenotype and genotype, with a prevalence of 1/3000 - 1/4000 in the general population.[1] RP can be inherited in an autosomal dominant, autosomal recessive or X-linked pattern.[1, 2] X-Linked RP (XLRP) cases account for 15% of males with simplex disease.[3] XLRP is a severe form of RP, with most affected males presenting with early-onset vision loss (<10 years of age), nyctalopia, nystagmus, severely abnormal or undetectable electroretinogram (ERG) and progression to legal blindness by the 3rd to 4th decade.[4-6] XLRP patients have symptomatic night blindness from early childhood and are often myopic. *RPGR* and *RP2* disease-causing variants are the commonest causes of XLRP accounting for 80-90% of cases.[1] The on-going gene therapy clinical trials for *RPGR*-associated XLRP[7] were preceded by multiple studies describing in depth characterization of disease natural history.[8-14] In contrast, the current literature describing the *RP2* phenotype is limited.

RP2 disease-causing variants are responsible for 5-20% of XLRP.[15-20] The reports comparing the severity of *RPGR* and *RP2* XLRP have been inconclusive as to which genotype is associated with worse prognosis.[2, 5, 6, 21, 22] The genotype-phenotype correlations in *RP2*-associated XLRP are limited.[23] Differential diagnosis of *RP2*- or *RPGR*-XLRP is challenging, since no ocular measurement is genotype-specific.[4, 5] A tapetal-like reflex can be observed both in patients and carriers with *RPGR*- and *RP2*-XLRP.[24]

RP2 (MIM 312600) is located on Xp11.23 and has a structure similar to cofactor C, which is involved in β-tubulin folding.[19] *RP2* encodes a GTPase-activating protein (GAP) for the small GTPase ARL3, and has a role in trafficking lipidated proteins in the retina to the outer segment of photoreceptors.[25, 26] Using retinal pigment epithelium (RPE) and 3D retinal organoids differentiated from patient-derived inducible pluripotent stem cells (iPSCs) with an *RP2* premature stop variant, read-through drugs and AAV gene therapy rescued the cellular phenotype, supporting a clinical trial in patients.[27, 28] However, there is currently a lack of robust natural history data in genetically proven patients with *RP2*-associated retinopathy. These data are needed to provide better informed advice on prognosis and optimize design of clinical trials including identifying possible robust outcome measures and participant stratification.

The current study thereby provides a detailed characterization of the clinical phenotype, molecular basis, and natural history of a large series of patients with *RP2* retinopathy.

METHODS

Subject identification and assessment

Males harboring disease-causing variants in *RP2* were identified from Moorfields Eye Hospital (London, UK) and University of Arkansas Medical Science (Little Rock, AR, USA) retinal genetics clinics. All patients included were previously informed and consented. This retrospective study adhered to the tenets of the Declaration of Helsinki and was approved by the local ethics committees.

Molecular diagnosis

The majority of patients were screened using a diagnostic targeted next generation sequencing panel for retinal dystrophy. Others were ascertained either via research based whole exome sequencing, or with targeted Sanger sequencing of *RP2*. Variants are annotated according to the Reference Sequence NM_006915. All variants have a gnomAD frequency of 0 (gnomAD v2.1.1). Splice site variants were assessed using SpliceAI (https://spliceailookup.broadinstitute.org).

Clinical notes

Clinical data extracted included age of onset, visual acuity, slit lamp biomicroscopy and fundoscopy findings. Symptoms at presentation and complications were also recorded. All available data were reviewed, including the findings at the last available follow-up.

Best Corrected Visual Acuity (BCVA) and Clinical severity grading

BCVA was assessed monocularly with Snellen chart and converted to logarithmic minimum angle of resolution (LogMAR) for statistical analysis. Jayasundera et al. have described an approach to subdivide *RP2*-XLRP patients into mild, less severe, and severe.[20] Patients with relatively late onset severe macular dysfunction were considered less severe. BCVA with different cut-offs for different age ranges, was used as a subjective surrogate for macular function. We adopted and adapted the same clinical severity grading criteria into LogMAR, and applied it for the best seeing eye (**Supplementary Table 1**).

In addition, BCVA of the best seeing eye was used to categorize patients into one of four groups based on the World Health Organization (WHO) visual impairment criteria, that defines a person with no or mild visual impairment when presenting VA is $\leq$ 0.48 LogMAR, moderate impairment when VA is 0.48 -1 LogMAR, severe if 1-1.3 LogMAR, and blindness if it is greater than 1.3 LogMAR (**Supplementary Table 1**). Low vision corresponds to patients with moderate and severe impairment. Counting fingers vision was given a value of LogMAR 1.98 and hand motion, LogMAR 2.28, light perception and no light perception were specified as LogMAR 2.7 and 3, respectively.[29] The BCVA classification criteria are summarized in **Supplementary Table 1**.

Electrophysiological testing

Pattern and full-field electroretinogram (PERG; ERG) testing was performed in 22 patients, incorporating the standards of the International Society for Clinical Electrophysiology of Vision (ISCEV).[30, 31] Pattern ERG P50 was used as an

objective measure of macular function and the full-field ERG used to assess generalised retinal function of rod and cone systems. The ERG data were compared with a reference range from a group of healthy subjects (age range: 10-79 years).[32, 33] The amplitudes of the main full-field ERG components were plotted as a percentage of the age-matched lower limit of normal or as a difference from the age-matched upper peak time limit, including the dark adapted (DA) 10 ERG a-wave, and the light-adapted (LA) 3 single flash ERG b-wave and the LA 3 30Hz ERG. To address non-Gaussian distribution within the control group, the limits were defined as the lowest amplitude value in the control group minus 5% of the reference range (maximum minus minimum values) for amplitudes or plus 5% of the reference range for peak times.[34, 35]

Fundus Autofluorescence (FAF)

FAF images were obtained using short-wavelength excitation (488 nm) and a scanning laser ophthalmoscope according to previously described methods.[36] Images were reviewed by one grader (MG) and qualitatively graded.

Optical Coherence Tomography (OCT)

The majority of patients seen over the last fifteen years had both OCT and FAF imaging. Horizontal scans acquired using the Heidelberg Spectralis OCT (Heidelberg Engineering, Heidelberg, Germany) were chosen for quantifying the residual ellipsoid zone width (EZW), using the foveal reflex as a reference point. In addition, the device was switched to follow-up mode, so that the same scanning location was imaged at the follow-up visit as the baseline. This enabled comparable measurements to be made between the two visits for a

given subject. In others, the analysis described by Tee et al.[37] was used to align locations for follow-up measurements of retinal thickness and the EZW (described in detail in **Supplementary Methods**). Vendor supplied Heidelberg Eye Explorer (Heyex) software version 1.6.1.0 was used for image analysis and quantification of EZW, employing the caliper tool.[38]

Statistical Analysis

Statistical analysis was carried out using SPSS Statistics for Windows (Version 22.0. Armonk, NY: IBM Corp.). Significance for all statistical tests was set at $P<0.05$. The Shapiro-Wilk test was used to test for normality for all variables.

RESULTS

Molecular Genetics

A total of 54 molecularly confirmed patients were identified, from 38 pedigrees. Twenty-eight variants were identified. The most common variant was c.358C>T p.(Arg120*), identified in 5 pedigrees (13%); 6 variants were identified in 2 pedigrees each and all others were restricted to single families. Identified variants included 8 frameshift alterations (28.6%), 7 missense (25.0%), 6 nonsense (21.4%) and 3 splice site changes (10.7%). One patient had a whole gene deletion and three patients had smaller deletions. Twenty of the variants, including the deletions, have not been previously clinically characterized. **Figure 1** shows the distribution of the variants across the *RP2* gene/protein.

Supplementary Table 2 details the identified variants including their predicted effect.

Phenotype, Age of Onset and Presenting Symptoms

Fifty-three patients (98.1%) presented with RP. Age of onset was documented for 48 patients. The mean age of onset (range, ±SD) was 9.6 years of age (1-57 years, ± 9.2 years). Forty-four patients (91.7%) had childhood-onset disease (age range 1-16 years old), with mean age of disease onset (±SD) of 7.6 years (±4.1 years). The four patients with adulthood-onset disease had mean age of onset 32.5 years (range: 17-57 years). One patient presented with symptoms and signs consistent with cone-rod dystrophy (CORD, 1.9%) with onset of symptoms at age 10 years.

The first symptom/s at disease onset were described in 48 of the patients with RP and included night blindness (n=33, 68.8%), decreased central vision (n=8, 16.7%), both night blindness and decreased central vision (n=4, 8.3%), decreased central vision and peripheral vision loss (n=2, 4.2%). One patient with RP presented with nystagmus (n=1, 2.1%). The patient with CORD presented with decreased central vision and developed night vision difficulties later in life. Clinical data are summarized in **Table 3**.

Genotype-phenotype correlations

Null and missense variants were present in childhood-onset and adult-hood onset groups. Of the four patients with adulthood-onset disease, two had frameshift variants with truncation/loss of function, one had a splice site variant with loss of donor splice site and one had a substitution. In the childhood-onset

group the phenotype was uniform, with early onset disease and early degeneration. No genotype-phenotype correlations were observed in the current report.

Best Corrected Visual Acuity (BCVA)

BCVA was documented in at least one visit for 53 patients and was reduced in all cases. Mean age (range, ±SD) for baseline BCVA for the whole cohort was 23.2 years (3.8-71, ±17.4 years), with a mean BCVA (range, ±SD) of 0.91 LogMAR (0-2.7, ±0.80) and 0.94 LogMAR (0-2.7, ±0.78) for right and left eyes respectively. Forty-three had available longitudinal data, with a mean follow-up (range, ±SD) of 7.3 years (0.3-30.2, ±7.1 years). Mean BCVA change was 0.37 and 0.29 Log MAR for right and left eyes, respectively for the follow-up period, and was not statistically significantly different between right and left eyes (paired t-test $P<0.05$). BCVA data are summarized in **Table 1** and mean baseline BCVA against age is presented in **Figure 2A**.

Disease Severity

Based on previously described clinical severity grading criteria (**Supplementary Table 1**): 21 patients had mild disease and 32 patients had severe disease at baseline. Of the 21 patients with mild disease, 18 were seen longitudinally. Eight of those 18 patients met the criteria for severe disease over a follow-up of 9.9 years (SD: ± 4.8, range: 3-15.1 years). The 10 patients with mild disease at the last follow-up visit, had significantly shorter follow-up time (mean ±SD: 4.8 ± 4.1 years), with three of them having later onset adulthood disease.

Based on the WHO visual impairment criteria: 24 patients (45%) had no or mild visual impairment, 11 patients (21%) had moderate impairment, 7 (13%) had severe impairment and 11 (21%) were blind. In total, 18 patients (34%) had low vision. **Figure 2B** depicts the age distribution for each class of visual impairment.

Non-Ocular Manifestations

No non-ocular manifestations were identified. However, ascertainment bias cannot be excluded, as the vast majority of patients were recruited from a stand-alone eye hospital (MEH).

Electrophysiology

There was high degree of inter-ocular ERG symmetry based on amplitudes of the DA 0.01, DA 3 and DA 10 ERG a- and b-waves, LA 30Hz ERG and LA 3 (single flash) ERG b-waves (slope = 0.94; r^2= 0.95) and on the peak times of the DA 10 ERG b-waves and LA 30Hz ERGs (slope = 1.1; r^2=0.86).

Three of 22 patients had undetectable full-field ERGs under all stimulus conditions (ages 8, 18 and 21 years) and 2 others showed severe and similar reductions of DA and LA ERGs, consistent with a severe rod and cone photoreceptor dystrophy. The majority (n=17), including the 11 with the mildest DA10 ERG a-wave reductions, showed better preservation of LA ERGs than DA 10 ERG a-waves, in keeping with a rod-cone dystrophy (**Figure 3**). All 17 patients with a detectable response showed delay in the LA 30Hz ERG, including the majority (n=13) with severe delays of between 10 and 24ms. Pattern ERG P50 was undetectable in all but 2 patients, including patient 12 (P50 delayed by 7ms and reduced by >70%; **Figure 4b**) and patient 21 (P50 delayed by 10ms and reduced by >25%; **Figure 4c**). **Figure 3** summarizes the electrophysiological findings and patient ages at the time of testing and **Figure 4** shows representative recordings.

There was no significant correlation between age and the amplitudes of the DA 0.01 ERG, DA 10 ERG a- and b-waves, LA 30Hz ERG or LA3 ERG b-

waves (maximum r^2 = 0.083) or the peak times of the LA 30Hz (r^2=0.025), although the narrow age range is highlighted (all but 1 patient were aged between 5 and 21 years). Serial data were available in one child from the age of 7 years and revealed progressive PERG P50 reduction over 5 years and marked worsening of the DA 10 ERG between the ages of 10 and 12 years (**Supplementary Figure 5**).

Fundus Autofluorescence (FAF)

FAF imaging was available for 46 patients for at least one visit. At first evaluation, the mean age (±SD, range) was 25.1 years (±16.7, 5.8-69.2 years). A range of FAF findings was observed, from normal FAF to advanced atrophy. **Figure 6** shows examples of the different patterns of FAF observed. On qualitative assessment we identified normal FAF in 11 patients (23.9%, mean age ±SD, range: 15.2 ±11.1, 5.8-46.2 years old). Two patients, aged 11 and 24 years, had a paracentral macular ring of increased signal; six patients (13%) had a macular ring of increased signal and mid-peripheral patchy changes with a mean age (±SD, range) of 18.71 (5.8, 11-25.9) years old; four patients had patchy macular signal and midperipheral changes (8.7%, mean age ±SD, range: 26.0 ±28.1, 6.7-68.2 years old); a further four patients had normal macular signal with patchy midperipheral changes (8.7%, mean age ±SD, range: 27.4 ±23.4, 12.2-62.1 years old), and one patient had patchy macular signal with normal periphery. Eighteen patients (39.1%) had atrophy at a mean age 34.0 years old (±15.1, 15.8-69.2). Three of the patients with advanced atrophy had a choroideremia-like pattern. Atrophy was the commonest pattern on FAF imaging and in total 31 patients (67.4%) had visible changes at the macula at baseline.

Follow-up FAF was available for thirty-six patients. The mean (±SD, range) follow-up time was 6.0 years (±4.3, 0.6-17.6 years). Nine of nine patients with normal FAF at baseline showed abnormal changes (mean follow-up period of 6.4 years). The FAF showed a high degree of inter-ocular symmetry in all cases, including those that had repeat imaging (examples shown in **Supplementary Figure 7)**.

Optical Coherence Tomography (OCT)

Forty-six patients had at least one OCT imaging session. Baseline age (±SD, range) was 27.2 years old (±17.5, 5.2-69.2 years). EZ width and ONL thickness was not statistically significantly different between right and left eye (paired t-test $P<0.05$). For further assessment, the mean EZW and ONL thickness for both eyes was calculated for each patient at each visit.

Forty-two of the 46 patients had childhood-onset disease. Twenty-three had no identifiable EZ and complete ONL thickness loss at mean age (±SD, range) of 36.4 years (±16.0, 17.9-69.2). Nineteen patients (mean age ±SD, range: 13.5 ±5.7, 5.3-25.9 years), had identifiable EZ and residual ONL thickness. Mean EZW was 1493 (±1496, 458-6280 µm) and mean ONL was 82 µm (31, 31-147 µm). **Figure 8** presents the distribution of EZW and ONL thickness with age. Sixteen of the patients with identifiable EZ and ONL, had longitudinal assessment, with a mean follow-up of 5.3 years. The mean annual rate of EZW loss was 219 µm/year and the mean annual decrease in ONL thickness was 4.93 µm/year. No patient with childhood-onset disease had identifiable EZ after the age of 26 years at baseline or follow-up. **Supplementary Figure 9** shows representative examples of OCT scans from 3 adult patients with complete EZ loss.

The four patients with adulthood-onset disease (mean age, range: 36.6, 20.5-68.2 years old) had evidence of a relatively preserved EZ (mean width 3255 µm, range 615-6500µm) and ONL (mean width: 89.63 µm, range: 64-129µm). Three of the four patients had longitudinal assessment after a mean follow-up of 3.9 years. The one patient with age of onset 17 years progressed to complete EZ loss over 7.4 years (age at follow-up: 31 years old). The two patients with later onset disease had stable imaging after 1.4 and 2.9 years (**Figure 10**).

DISCUSSION

This study details the clinical phenotype in the largest cohort of genetically characterized patients with *RP2*-associated retinopathy to date, including novel genetic findings. Comprehensive electrophysiological testing, natural history and serial retinal imaging data highlight the structural and functional spectrum and variability of the disease, with the aim of informing future patient management and interventional trials. *RP2*-retinopathy is a predominantly childhood-onset, rapidly progressive retinal degeneration, with macular involvement and early complete loss of EZ in most cases.

In contrast with some other forms of progressive IRDs,[39, 40] there was less dissociation of structure and central vision; central vision was severely decreased in all patients with childhood-onset disease and the OCT EZ was undetectable by the age of 26 years in most cases. Electrophysiological testing also revealed PERG evidence of macular dysfunction, severe in all but two cases. Full-field ERGs were mostly consistent with rod-cone dystrophy but the severity of generalized (mainly peripheral) retinal dysfunction varied greatly in children and adolescents of a similar age, ranging from undetectable (severe rod and cone photoreceptor dystrophy) to near-normal cone-mediated ERG components (**Figure 3**).

Rare exceptions of adulthood-onset disease with relative preservation of outer retinal structure (**Figure 10**) and the wide range of ERG abnormalities in patients of a similar age (**Figure 3**), highlight the necessity of individual assessments, important to the selection of candidates most suitable for clinical trials and possible future treatment. Patients with complete loss of EZ and geographic atrophy, irrespective of age, are less likely to benefit from attempts

to rescue/regain macular function or to arrest progressive maculopathy. There was a rapid rate of progressive EZW reduction and decline in ONL thickness, highlighting a relatively narrow window for intervention. Although clinically significant structural changes are likely to be observed within a short time frame in a clinical trial. However, the severity of degeneration may impose challenges in the accurate measurement of such changes.

In the current cohort we identified three patients with a choroideremia-like phenotype similar to some older patients described in a previous study of XLRP,[20] with advanced degeneration and of older age. It should be noted that none of those patients had a preserved island of vision and the choriocapillaris atrophy may represent changes secondary to the chronic retinal atrophy. Those cases may highlight the potential value of functional rescue of peripheral retinal function in cases with severe maculopathy, particularly given that some may have near-normal or relatively preserved cone-mediated ERGs (**Figure 3**).

Ideally, future prospective studies with standardized imaging acquisition protocols need to establish the inter-session repeatability of measurements before being employed as outcome measurements in trials. Also the use of novel high-resolution imaging techniques such as adaptive optics scanning laser ophthalmoscopy may be more sensitive to change.[41] Prospective natural history studies that monitor patients from a young age will be vital to better establish prognosis, phenotype-genotype correlations and meaningful endpoints for trials. Such studies can inform the design of planned treatment trials, including recruitment criteria, assesments and follow-up time. The pre-clinical work performed both assessing gene therapy, as well as read-through drugs make *RP2*-retinopathy an attractive target for intervention.[42]

The retrospective nature of the current study has inherent limitations. Follow-up intervals were not standardized and the functional assesments did not include visual field testing. Further investigation of female carriers that manifest retinal disease will be of value, in order to determine disease severity and inform counselling; moreover, they may also be candidates for intervention.[24]

This report of a large *RP2*-associated retinal dystrophy cohort helps to define the phenotypic and genetic spectrum. The disorder is characterized by childhood-onset retinal degeneration usually with early macular involvement. Full-field ERGs reveal rod-cone dystrophy in the vast majority, with generalized (peripheral) cone system involvement of widely varying severity in the first two decades of life, and OCT imaging shows early complete EZ loss. Novel therapies for *RP2* are under advanced development and clinical trials are anticipated in the near future. The findings of this study will inform patient management and counselling and are pertinent to the appropriate selection of patients in future clinical trials.

FOOTNOTES

Financial Disclosure(s): MM consult for MeiraGTx.

This work was supported by grants from the National Institute for Health Research Biomedical Research Centre at Moorfields Eye Hospital National Health Service Foundation Trust and UCL Institute of Ophthalmology, and the The Wellcome Trust (099173/Z/12/Z).

Contributors: MG and AR analyzed the data and drafted the manuscript. MG, SHU, MM, AW and AJH conceived, supervised, and revised the manuscript. All authors provided critical revision of the manuscript.

Competing interests: None declared.

Provenance and peer review: Not commissioned; externally peer reviewed.

Obtained funding: N/A

Overall Responsibility: MG, AGR, AJH and MM

LEGENDS

Figure 1: Schematic representation of variants in the *RP2* gene and protein.

The identified variants are marked along the corresponding location of the *RP2* gene and protein. Black shaded boxes represent the coding exons (exons 1 to 5) separated by introns (solid line), with the protein domains (bottom panel) coded by each exon indicated with a dotted line.

Figure 2: Visual Impairment

(A) Scattered plot graph presenting mean baseline best corrected visual acuity (BCVA) against age, and (B) stacked scatter plot depicts the age distribution among the different categories of visual impairment based on World Health Organization classification. As expected a greater degree of impairment was present in older patients, with the exception of patients with adulthood-onset disease (open diamonds).

Figure 3: Full field ERG

Full field ERG findings summarized in 22 subjects tested according to the ISCEV standard methods; a) The amplitudes of the DA0.01 ERG, DA 10 ERG a-wave, LA 30 Hz ERG and LA 3 ERG b-wave are plotted against the primary axis as a percentage of the age-matched lower limit of the ("normal") reference range (horizontal broken line), with values arranged in ascending order of DA10 ERG a-wave amplitude for clarity. The LA 30 Hz peak times are plotted as a difference from the age-matched upper limit of normal timing (horizontal dotted line) against the secondary axis. b) The age of the patients at the time of testing, arranged in same order as in a).

Figure 4: Representative full-field and pattern ERGs

Patient 4 (a; aged 13 years), 12 (b; 13 years) and 21 (c; 7 years) correspond to the patient numbering used in **Figure 3**. Representative control ("normal") recordings are shown for comparison (d). Data are shown for the right eyes

only, as all showed a high degree of inter-ocular symmetry. Patient traces are superimposed to demonstrate reproducibility. Broken lines replace blink artefacts for clarity. In all 3 patients there is ERG evidence of rod-cone dystrophy. Pattern ERG P50 abnormalities are consistent with macular involvement that is a) severe, b) moderate or c) relatively mild.

Figure 6: Fundus Autofluorescence (FAF) Imaging

FAF imaging of six patients with *RP2*-associated retinopathy at different stages of the disease. (A) Normal pattern of autofluorescence. (B) Midperipheral patchy signal, with early patchy foveal pattern. (C) Midperipheral patchy signal, with increased foveal signal. (D) Foveal atrophy, without midperipheral changes. (E) Midperipheral patchy signal, with foveal atrophy. (F) Diffuse atrophic changes.

Figure 8: Optical Coherence Tomography (OCT) Graphs

Scattered plots presenting (A) ellipsoid zone width (EZW) and age, and (B) outer nuclear layer (ONL) and age. Greater degree of impairment of structural loss is present in older patients, except for patients with adulthood-onset disease (open diamonds). No patient with childhood-onset disease had identifiable EZ or ONL after the third decade of life.

Figure 10: Optical Coherence Tomography (OCT) Imaging

OCT imaging of two patients with *RP2*-associated retinopathy with (A) childhood-onset disease, and (B) adulthood-onset disease. (A) Patient shows progressive loss of the ellipsoid zone over a follow-up of seven years, with no identifiable EZ by the age of 22 years old. (B) Patient had a well-preserved ellipsoid zone at age 46 years old and no ellipsoid zone loss was observed over three years of follow-up.

REFERENCES

1. Hartong DT, Berson EL, Dryja TP. Retinitis pigmentosa. Lancet 2006;368(9549):1795-809.
2. Tee JJ, Smith AJ, Hardcastle AJ, Michaelides M. RPGR-associated retinopathy: clinical features, molecular genetics, animal models and therapeutic options. Br J Ophthalmol 2016;100(8):1022-7.
3. Branham K, Othman M, Brumm M, et al. Mutations in RPGR and RP2 account for 15% of males with simplex retinal degenerative disease. Invest Ophthalmol Vis Sci 2012;53(13):8232-7.
4. Flaxel CJ, Jay M, Thiselton DL, et al. Difference between RP2 and RP3 phenotypes in X linked retinitis pigmentosa. Br J Ophthalmol 1999;83(10):1144-8.
5. Sharon D, Sandberg MA, Rabe VW, et al. RP2 and RPGR mutations and clinical correlations in patients with X-linked retinitis pigmentosa. Am J Hum Genet 2003;73(5):1131-46.
6. Sharon D, Bruns GA, McGee TL, et al. X-linked retinitis pigmentosa: mutation spectrum of the RPGR and RP2 genes and correlation with visual function. Invest Ophthalmol Vis Sci 2000;41(9):2712-21.
7. Georgiou M, Awadh Hashem S, Daich Varela M, Michaelides M. Gene Therapy in X-linked Retinitis Pigmentosa Due to Defects in RPGR. Int Ophthalmol Clin 2021;61(4):97-108.
8. Tee JJL, Yang Y, Kalitzeos A, et al. Natural History Study of Retinal Structure, Progression and Symmetry Using Ellipzoid Zone Metrics in RPGR-Associated Retinopathy. Am J Ophthalmol 2018.
9. Tee JJL, Yang Y, Kalitzeos A, et al. Characterization of Visual Function, Interocular Variability and Progression Using Static Perimetry-Derived Metrics in RPGR-Associated Retinopathy. Invest Ophthalmol Vis Sci 2018;59(6):2422-36.
10. Tee JJL, Carroll J, Webster AR, Michaelides M. Quantitative Analysis of Retinal Structure Using Spectral-Domain Optical Coherence Tomography in RPGR-Associated Retinopathy. Am J Ophthalmol 2017;178:18-26.
11. Talib M, van Schooneveld MJ, Thiadens AA, et al. CLINICAL AND GENETIC CHARACTERISTICS OF MALE PATIENTS WITH RPGR-ASSOCIATED RETINAL DYSTROPHIES: A Long-Term Follow-up Study. Retina 2018.
12. Cideciyan AV, Charng J, Roman AJ, et al. Progression in X-linked Retinitis Pigmentosa Due to ORF15-RPGR Mutations: Assessment of Localized Vision Changes Over 2 Years. Invest Ophthalmol Vis Sci 2018;59(11):4558-66.
13. Bellingrath JS, Ochakovski GA, Seitz IP, et al. High Symmetry of Visual Acuity and Visual Fields in RPGR-Linked Retinitis Pigmentosa. Invest Ophthalmol Vis Sci 2017;58(11):4457-66.
14. Anikina E, Georgiou M, Tee J, et al. Characterization of Retinal Function Using Microperimetry-Derived Metrics in Both Adults and Children With RPGR-Associated Retinopathy. Am J Ophthalmol 2022;234:81-90.
15. Breuer DK, Yashar BM, Filippova E, et al. A comprehensive mutation analysis of RP2 and RPGR in a North American cohort of families with X-linked retinitis pigmentosa. Am J Hum Genet 2002;70(6):1545-54.
16. Miano MG, Testa F, Filippini F, et al. Identification of novel RP2 mutations in a subset of X-linked retinitis pigmentosa families and prediction of new domains. Hum Mutat 2001;18(2):109-19.

17. Buraczynska M, Wu W, Fujita R, et al. Spectrum of mutations in the RPGR gene that are identified in 20% of families with X-linked retinitis pigmentosa. Am J Hum Genet 1997;61(6):1287-92.
18. Hardcastle AJ, Thiselton DL, Van Maldergem L, et al. Mutations in the RP2 gene cause disease in 10% of families with familial X-linked retinitis pigmentosa assessed in this study. Am J Hum Genet 1999;64(4):1210-5.
19. Schwahn U, Lenzner S, Dong J, et al. Positional cloning of the gene for X-linked retinitis pigmentosa 2. Nat Genet 1998;19(4):327-32.
20. Jayasundera T, Branham KE, Othman M, et al. RP2 phenotype and pathogenetic correlations in X-linked retinitis pigmentosa. Arch Ophthalmol 2010;128(7):915-23.
21. Friedrich U, Warburg M, Jorgensen AL. X-inactivation pattern in carriers of X-linked retinitis pigmentosa: a valuable means of prognostic evaluation? Hum Genet 1993;92(4):359-63.
22. Comander J, Weigel-DiFranco C, Sandberg MA, Berson EL. Visual Function in Carriers of X-Linked Retinitis Pigmentosa. Ophthalmology 2015;122(9):1899-906.
23. Rosenberg T, Schwahn U, Feil S, Berger W. Genotype-phenotype correlation in X-linked retinitis pigmentosa 2 (RP2). Ophthalmic Genet 1999;20(3):161-72.
24. De Silva SR, Arno G, Robson AG, et al. The X-linked retinopathies: Physiological insights, pathogenic mechanisms, phenotypic features and novel therapies. Prog Retin Eye Res 2020:100898.
25. Zhang H, Hanke-Gogokhia C, Jiang L, et al. Mistrafficking of prenylated proteins causes retinitis pigmentosa 2. Faseb j 2015;29(3):932-42.
26. Schwarz N, Lane A, Jovanovic K, et al. Arl3 and RP2 regulate the trafficking of ciliary tip kinesins. Hum Mol Genet 2017;26(13):2480-92.
27. Schwarz N, Carr AJ, Lane A, et al. Translational read-through of the RP2 Arg120stop mutation in patient iPSC-derived retinal pigment epithelium cells. Hum Mol Genet 2015;24(4):972-86.
28. Lane A, Jovanovic K, Shortall C, et al. Modeling and Rescue of RP2 Retinitis Pigmentosa Using iPSC-Derived Retinal Organoids. Stem Cell Reports 2020;15(1):67-79.
29. Lange C, Feltgen N, Junker B, et al. Resolving the clinical acuity categories "hand motion" and "counting fingers" using the Freiburg Visual Acuity Test (FrACT). Graefes Arch Clin Exp Ophthalmol 2009;247(1):137-42.
30. Bach M, Brigell MG, Hawlina M, et al. ISCEV standard for clinical pattern electroretinography (PERG): 2012 update. Doc Ophthalmol 2013;126(1):1-7.
31. Robson AG, Frishman LJ, Grigg J, et al. ISCEV Standard for full-field clinical electroretinography (2022 update). Doc Ophthalmol 2022;144(3):165-77.
32. Georgiou M, Robson AG, Fujinami K, et al. KCNV2-associated Retinopathy: Genetics, Electrophysiology and Clinical Course - KCNV2 Study Group Report 1. Am J Ophthalmol 2020.
33. de Carvalho ER, Robson AG, Arno G, et al. Enhanced S-Cone Syndrome: Spectrum of Clinical, Imaging, Electrophysiologic, and Genetic Findings in a Retrospective Case Series of 56 Patients. Ophthalmol Retina 2020.
34. Georgiou M, Robson AG, Singh N, et al. Deep Phenotyping of PDE6C-Associated Achromatopsia. Invest Ophthalmol Vis Sci 2019;60(15):5112-23.

611 35. Vincent A, Robson AG, Neveu MM, et al. A phenotype-genotype correlation
612 study of X-linked retinoschisis. Ophthalmology 2013;120(7):1454-64.
613 36. Georgiou M, Kane T, Tanna P, et al. Prospective Cohort Study of
614 Childhood-Onset Stargardt Disease: Fundus Autofluorescence Imaging,
615 Progression, Comparison with Adult-Onset Disease, and Disease Symmetry. Am J
616 Ophthalmol 2019.
617 37. Tee JJL, Kalitzeos A, Webster AR, et al. QUANTITATIVE ANALYSIS OF
618 HYPERAUTOFLUORESCENT RINGS TO CHARACTERIZE THE NATURAL HISTORY
619 AND PROGRESSION IN RPGR-ASSOCIATED RETINOPATHY. Retina 2017.
620 38. Ramachandran R, C XC, Lee D, et al. Reliability of a Manual Procedure for
621 Marking the EZ Endpoint Location in Patients with Retinitis Pigmentosa. (2164-
622 2591 (Print)).
623 39. Bouzia Z, Georgiou M, Hull S, et al. GUCY2D-Associated Leber Congenital
624 Amaurosis: A Retrospective Natural History Study in Preparation for Trials of
625 Novel Therapies. Am J Ophthalmol 2020;210:59-70.
626 40. Kumaran N, Georgiou M, Bainbridge JWB, et al. Retinal Structure in
627 RPE65-Associated Retinal Dystrophy. Invest Ophthalmol Vis Sci 2020;61(4):47.
628 41. Georgiou M, Kalitzeos A, Patterson EJ, et al. Adaptive optics imaging of
629 inherited retinal diseases. Br J Ophthalmol 2018;102(8):1028-35.
630 42. Georgiou M, Fujinami K, Michaelides M. Inherited retinal diseases:
631 Therapeutics, clinical trials and end points-A review. Clin Exp Ophthalmol 2021.
632

Table 1: Clinical Data and Visual Impairment in *RP2*-Rod-Cone Dystrophy

Parameter-Characteristic		
Age of Onset	**(n=)**	**Mean (±SD Range,)**
Rod-Cone Dystrophy	48	9.63 ± 9.20, 1-57 years
Childhood-Onset	44 (91.7%)	7.55 ± 4.10,1-16 years
Adulthood-Onset	4 (8.3%)	32.5 ± 16.15, 17-57 years
Presenting Symptoms*		
Night Blindness	33 (68.8%)	
Decreased Central Vision	8 (16.7%)	
Night Blindness and Decreased Central Vision	4 (8.3%)	
Decreased Central and Peripheral Vision	2 (4.2%)	
Nystagmus	1 (2.1%)	
Best Corrected Visual Acuity (BCVA)		
Age at Baseline, n=53		23.2 ± 17.4, 3.8-71 years
Right Eye Mean BCVA at Baseline		0.91 ±0.80, 0-2.7 LogMAR
Left Eye BCVA at Baseline		0.94 ±0.78 0-2.7 LogMAR
Mean Follow-up, n=43		7.3 ±7.1, 0.3-30.2 years
Right Eye BCVA at Follow-up		1.17 ±0.84, 0.16-3.0 LogMAR
Left Eye BCVA at Follow-up		1.16 ±0.78, 0.16-3.0 LogMAR
Disease Severity		
Baseline, n=53		
Mild Disease	21 (39.6%)	
Severe Disease	32 (60.4%)	
Follow-up, n=50		
Mild Disease	10 (20%)	
Severe Disease	40 (80%)	
WHO Visual Impairment		
No or mild visual impairment	24 (45%)	
Moderate impairment	11 (21%)	
Severe impairment	7 (13%)	
Blindness	11 (21%)	

***The single patient with cone-rod dystrophy presented with decreased central vision.**

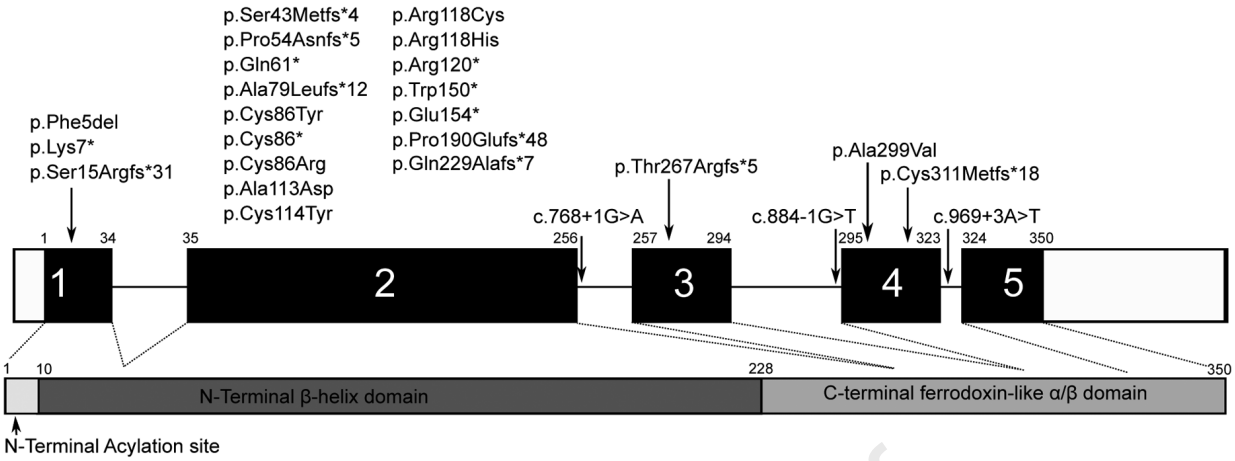

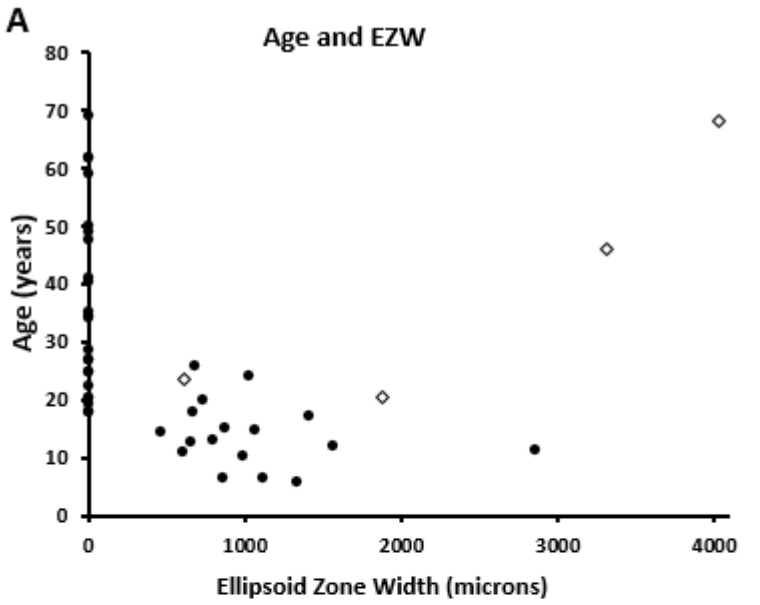

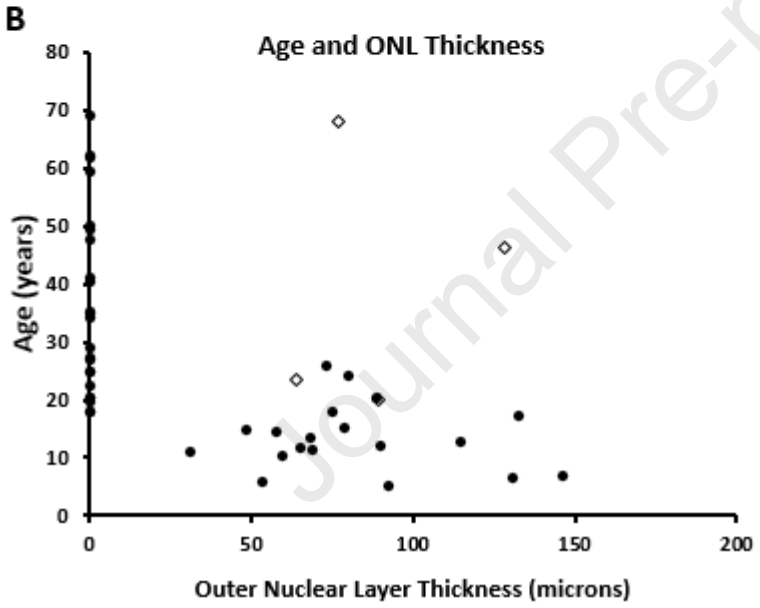

a.

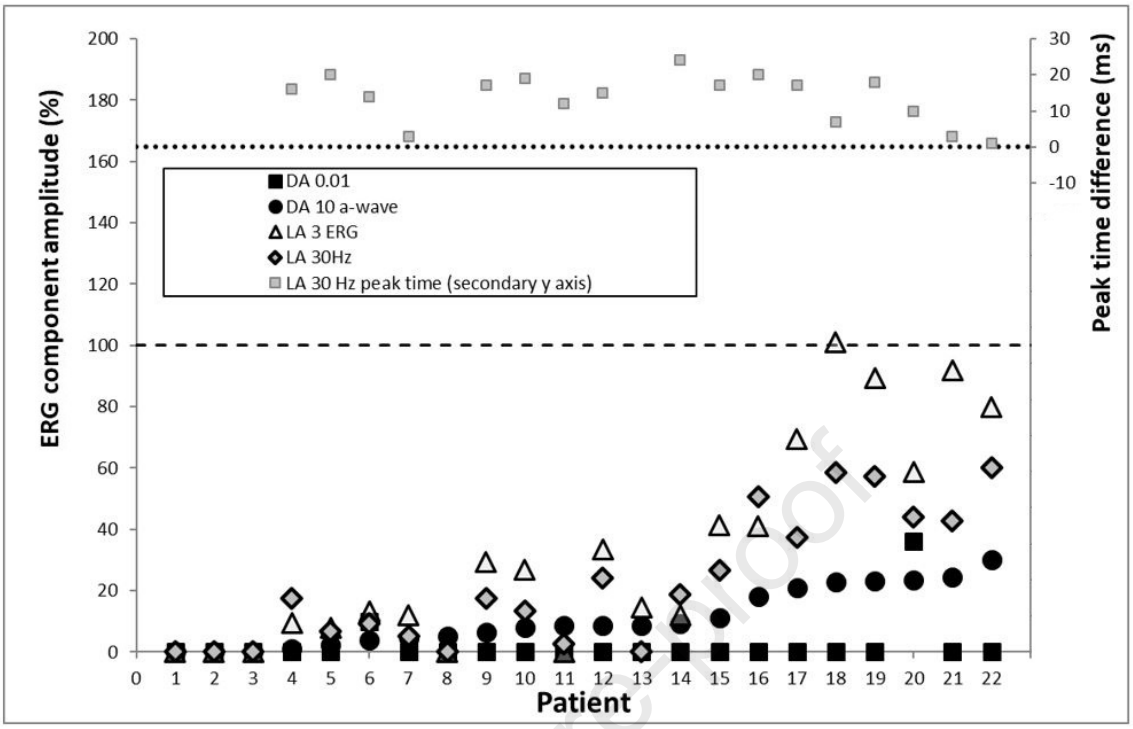

b.

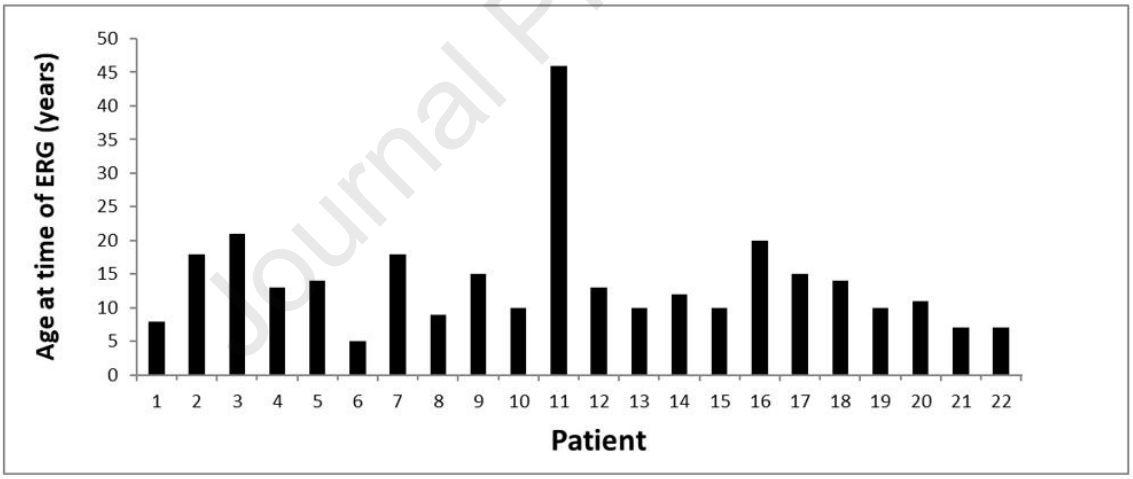

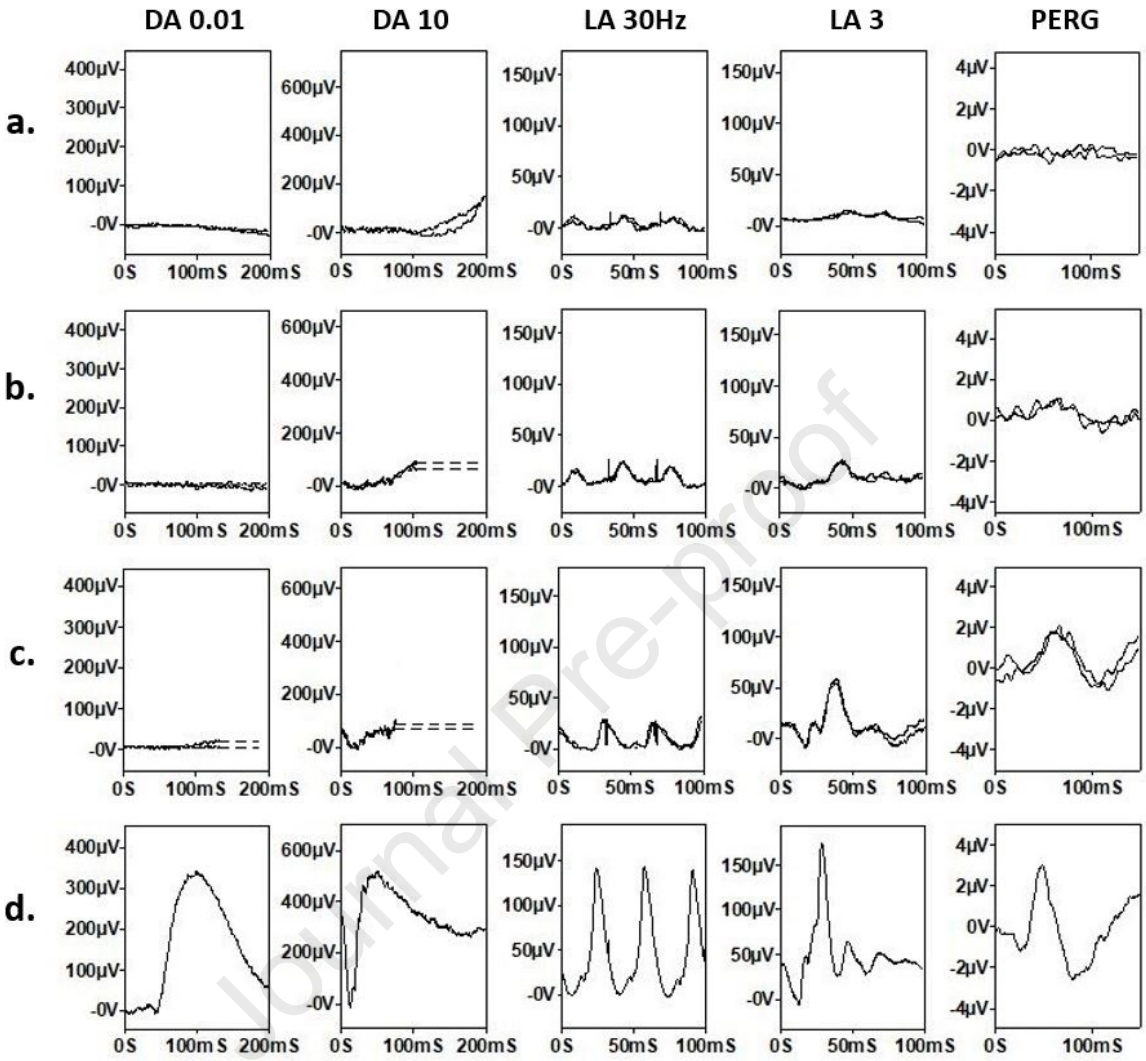

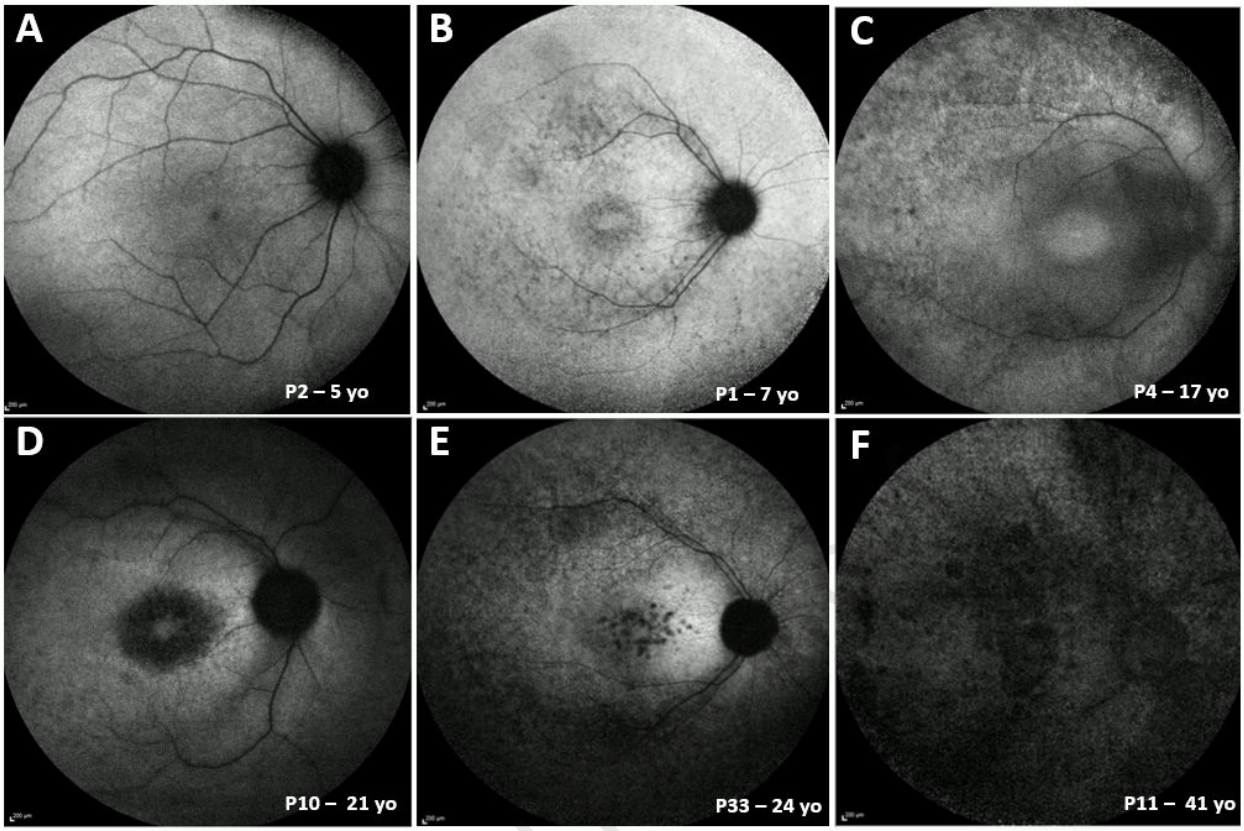

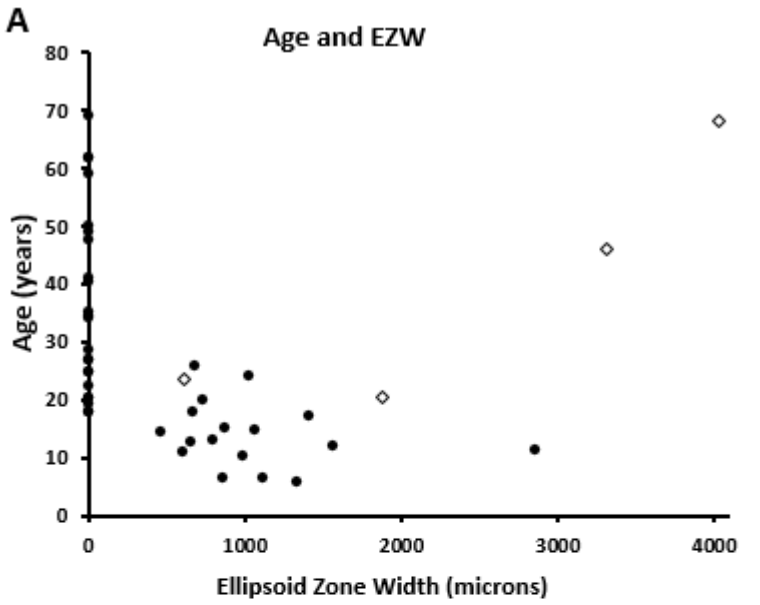

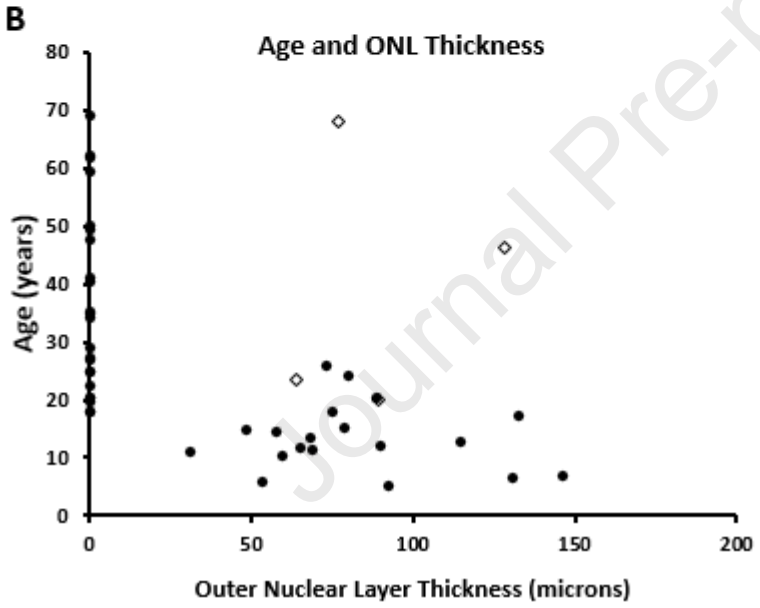

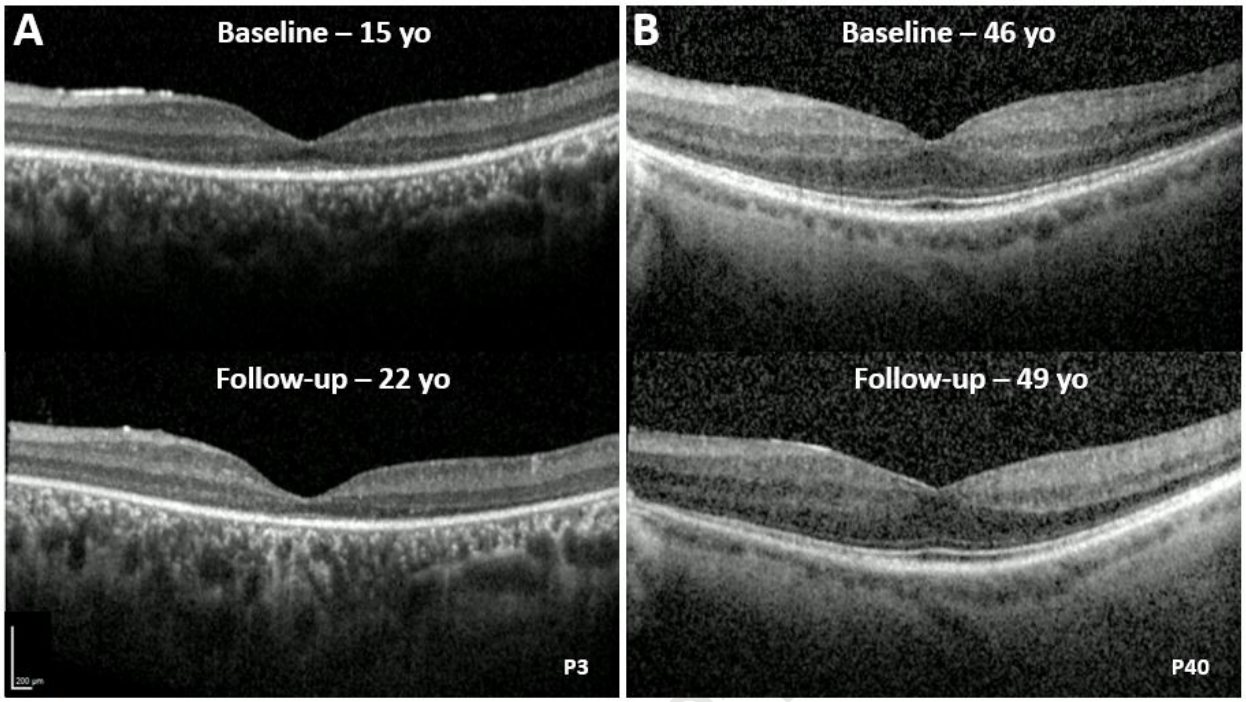

Precis

Deep phenotyping of the functional and anatomical characteristics of patients with *RP2*-associated retinopathy, in a large cohort, in preparation for planned novel therapeutic interventions.